Journal of Quantitative Spectroscopy & Radiative Transfer 176 (2016) 129–136

Contents lists available at ScienceDirect

Journal of Quantitative Spectroscopy & Radiative Transfer

journal homepage: www.elsevier.com/locate/jqsrt

Full-spectrum *k*-distribution look-up table for nonhomogeneous gas–soot mixtures

Chaojun Wang [a,b], Michael F. Modest [b,*], Boshu He [a]

[a] School of Mechanical, Electronic and Control Engineering, Beijing Jiaotong University, Beijing, China
[b] School of Engineering, University of California, Merced, USA

ARTICLE INFO

Article history:
Received 22 September 2015
Received in revised form
16 December 2015
Accepted 3 February 2016
Available online 2 March 2016

Keywords:
Full-spectrum *k*-distribution
Look-up table
Soot
Optimization

ABSTRACT

Full-spectrum *k*-distribution (FSK) look-up tables provide great accuracy combined with outstanding numerical efficiency for the evaluation of radiative transfer in nonhomogeneous gaseous media. However, previously published tables cannot be used for gas–soot mixtures that are found in most combustion scenarios since it is impossible to assemble *k*-distributions for a gas mixed with nongray absorbing particles from gas-only full-spectrum *k*-distributions. Consequently, a new FSK look-up table has been constructed by optimizing the previous table recently published by the authors and then adding one soot volume fraction to this optimized table. Two steps comprise the optimization scheme: (1) direct calculation of the nongray stretching factors (*a*-values) using the *k*-distributions (*k*-values) rather than tabulating them; (2) deletion of unnecessary mole fractions at many thermodynamic states. Results show that after optimization, the size of the new table is reduced from 5 GB (including the *k*-values and the *a*-values for gases only) to 3.2 GB (including the *k*-values for both gases and soot) while both accuracy and efficiency remain the same. Two scaled flames are used to validate the new table. It is shown that the new table gives results of excellent accuracy for those benchmark results together with cheap computational cost for both gas mixtures and gas–soot mixtures.

1. Introduction

Accurate evaluation of nongray radiative properties, such as gas and soot, is of great importance in the study of combustion of hydrocarbon fuels. The line-by-line (LBL) calculations can most accurately predict radiative properties in participating media [1], but are often not practical because of the large computational effort they require. Therefore, the LBL method is used only for benchmark solutions to validate approximate methods. To accurately and efficiently obtain nongray radiative properties, Modest [2] developed the full-spectrum *k*-distribution (FSK) method based on the reordering concept. Recently, Wang et al. [3] constructed an FSK look-up table (old table) for mixtures of CO_2, H_2O and CO, which can achieve the LBL accuracy, but at a tiny fraction of the LBL computational cost.

However, in most combustion scenarios, gases are not the only radiatively participating media; soot particles, generated during combustion processes, play a very important role in radiation, but for which the old table valid only for gaseous media cannot be used. Unlike the oscillatory absorption coefficients of gases that can be treated as statistically independent random variables, the absorption coefficients of soot show a monotonic trend with wavenumber, and accurate *k*-distributions of gas–soot mixtures cannot be obtained by directly mixing soot *k*-distributions and gas *k*-distributions from the old table. To relax this limitation, Modest et al. [4] proposed that the gas–soot mixture full-spectrum *k*-distributions can be assembled at the narrow-band level. However, due to

* Corresponding author. Fax: +1 209 228 4047.
E-mail address: mmodest@eng.ucmerced.edu (M.F. Modest).

http://dx.doi.org/10.1016/j.jqsrt.2016.02.007
0022-4073/

Nomenclature

a	nongray stretching factor in FSK method (-)
E	total emission (kW/m^3)
f	full-spectrum k-distribution (cm)
f_v	soot volume fraction (-)
g	cumulative full-spectrum k-distribution or quadrature point (-)
I	radiative intensity (W/(m^2 sr))
k	absorption coefficient variable (cm^{-1})
m	complex index of refraction (-)
p	total pressure (bar)
T	temperature (K)
x	mole fraction (-)

Greek symbols

η	wavenumber (cm^{-1})
λ	wavelength (μm)
κ	absorption coefficient (cm^{-1})
$\underline{\phi}$	vector of local thermodynamic state variables

Subscripts

b	blackbody
p	pressure-based

Superscripts

0	reference state

Abbreviations

FSK	full-spectrum k-distribution
LBL	line-by-line
RTE	radiative transfer equation

mixing and assembly, the computational time requirements are 3 orders of magnitude higher than those for a look-up table [3].

The purpose of this technical note is to extend the applicability range of the old table from gaseous media to gas–soot mixtures, which is achieved in two steps: (1) optimizing the old table by eliminating all the a-values as well as the unnecessary mole fractions at different thermodynamic states; (2) constructing a new FSK look-up table (new table) based on the optimized table by adding one soot volume fraction. Two scaled flames are used to demonstrate the accuracy of the new table as well as the superior efficiency for radiative calculations in both gas and gas–soot mixtures.

2. Theoretical background

2.1. Full-spectrum k-distribution

Since this technical note is a supplement to [3], the theoretical background about the FSK used here are the same as those used in [3]. For simplification, here only the essential formulations are reviewed and additional details can be found in [3].

A full-spectrum k-distribution accounts for the variations of the Planck function and is defined as [5]

$$f(k;\underline{\phi},T)=\frac{1}{I_b(T)}\int_0^{\infty} I_{b\eta}(T)\delta(k-\kappa_\eta(\underline{\phi}))d\eta \tag{1}$$

where, κ_η is the absorption coefficient calculated from a spectroscopic database; $\delta(\cdot)$ is the Dirac-delta function; $\underline{\phi}$ is a vector of local thermodynamic state variables including pressure, temperature and species concentrations; $f(k;\underline{\phi},T)$ is a Planck-function-weighted k-distribution with the absorption coefficient evaluated at the local state $\underline{\phi}$ and a Planck function temperature T; $I_b(T)$ and $I_{b\eta}(T)$ are the Planck function and the spectral Planck function, respectively, at temperature T; and η is the wavenumber.

The cumulative full-spectrum k-distribution is defined as

$$g(k;\underline{\phi},T)=\int_0^k f(k';\underline{\phi},T)dk' \tag{2}$$

Thus, g represents the fraction of the spectrum whose absorption coefficient lies below the value of k and therefore, $0\le g\le 1$. Inverting Eq. (2), a smooth, monotonically increasing function $k(g)$ can be obtained, with the minimum and maximum values identical to those of κ_η.

2.2. Radiative properties of soot particles

Strongly radiating soot is generated in almost all combustion applications. In furnaces and boilers, the generation of soot is even necessary as a radiation source for efficient heat transfer. Soot is not a uniquely defined substance and normally can be regarded as a cloud of nonuniform-size small particles. Therefore, the absorption coefficient of soot particles can be determined using the small particle limit of Rayleigh scattering as [5]

$$\kappa_\lambda=\frac{36\pi n_s k_s}{(n_s^2-k_s^2+2)^2+4n_s^2k_s^2}\frac{f_v}{\lambda} \tag{3}$$

where, f_v is the volume fraction of soot particles; λ is the wavelength; n_s and k_s are the two parts of the soot's complex index of refraction m ($m=n_s-ik_s$), which are generally modeled using the correlation developed by Chang and Charalampopoulos [6],

$$n_s=1.811+0.1263\ln\lambda+0.027\ln^2\lambda+0.0417\ln^3\lambda \tag{4}$$

$$k_s=0.5281+0.1213\ln\lambda+0.2309\ln^2\lambda-0.01\ln^3\lambda \tag{5}$$

3. Construction of the new FSK look-up table

3.1. Optimization of the current FSK look-up table

3.1.1. Nongray stretching factor (a-values)

In nonhomogeneous media, the integral of the k-distribution over g-space is evaluated at a reference state $\underline{\phi}^0$. This leads to a parameter named the nongray stretching factor (a-values), defined as the ratio of any two full-spectrum k-distributions evaluated at the different Planck function temperatures, and can be expressed as

$$a(g^0;T,T^0)=\frac{f(k;\underline{\phi}^0,T)}{f(k;\underline{\phi}^0,T^0)}=\frac{dg(k;\underline{\phi}^0,T)}{dg(k;\underline{\phi}^0,T^0)} \tag{6}$$

In the old table, the k-values as well as the a-values at every thermodynamic state are all tabulated in the database. From Eq. (6), the a-values can also easily be directly calculated from two g-spaces corresponding to the same k. Since 32 Gauss–Chebyshev quadrature points were chosen as fixed g-values for all full-spectrum k-distributions in the database, directly calculating the a-values requires one more interpolation,

$$g(k_L;\underline{\phi}^0,T)\rightarrow g(k_R;\underline{\phi}^0,T) \tag{7}$$

where, k_L is the k-value evaluated at the reference state and the Planck function temperature T and k_R is the k-value evaluated at the reference state and the reference temperature T^0. Then, the a-values can be calculated from Eq. (6) as,

$$a({g_i}^0;T,T^0)=\frac{dg(k_{R,i};\underline{\phi}^0,T)}{dg(k_{R,i};\underline{\phi}^0,T^0)}\simeq\frac{g(k_{R,i+1};\underline{\phi}^0,T)-g(k_{R,i-1};\underline{\phi}^0,T)}{g(k_{R,i+1};\underline{\phi}^0,T^0)-g(k_{R,i-1};\underline{\phi}^0,T^0)} \tag{8}$$

where, i is the index of quadrature. Instead of tabulating the a-values, they may be obtained efficiently from Eq. (8), reducing the size of the FSK look-up table by half, from 5 GB to 2.5 GB. In radiative calculations, the a-values are only employed to calculate the total emission, which can be expressed as

$$E(T)=I_b(T)\int_0^1 k(g)a(g)dg \tag{9}$$

Since I_b is a constant at a specific temperature, the integral of Eq. (9) is used here to verify the accuracy of the a-values calculated by Eqs. (7) and (8). Table 1 lists comparisons of integrals using the tabulated a-values and the calculated a-values at different thermodynamic states. The k-values for those cases are all obtained from the old table. The error is found never exceeding 3%, implying that a-values can be obtained accurately from the corresponding k-values using Eqs. (7) and (8). Even though one more interpolation is required to calculate the a-values, there is no extra computational cost since linear interpolations are always needed to get the a-values from the tabulated database.

3.1.2. Unnecessary mole fractions

To decrease the nonlinear effects due to mixing and self-broadening, a large number of mole fractions are included in the old table. However, nonlinear effects vary with pressure, gas temperature, reference temperature and even quadrature point. At some thermodynamic states where there are very weak nonlinear effects, it is unnecessary to database so many mole fractions. Therefore, an optimized scheme was developed to delete unnecessary mole fractions at different thermodynamic states. The core concept of the optimization is to compare the tabulated values and the interpolated values. After setting the mole fractions of the other two species and the thermodynamic state with fixed pressure, Planck temperature and gas temperature, whether a tabulated mole fraction of the third species, x_j, may be eliminated is determined by checking both of the absolute error (AE) and the relative error (RE) for an interpolated value for $k_i(x_j)$, in terms of surrounding concentrations, $x_{j-1}<x_j<x_{j+1}$, where i denotes one of the 32 g-quadrature points for the k-distributions. The AE and the RE are evaluated as

$$\mathrm{AE}_i=\underbrace{k_i(x_j)}_{\text{Tabulated value}}-\underbrace{\left[(1-w)k_i(x_{j-1})+wk_i(x_{j+1})\right]}_{\text{Interpolated value}};\ w=\frac{x_j-x_{j-1}}{x_{j+1}-x_{j-1}}\quad \mathrm{RE}_i=\frac{\mathrm{AE}_i}{k_i(x_j)}\times 100\% \tag{10}$$

If $\mathrm{AE}_i<10^{-4}\mathrm{cm}^{-1}$ or $\mathrm{RE}_i<0.5\%$ for at least half of all 32 quadrature points, and also for at least 8 of the 16 larger quadrature points, the mole fraction x_j is eliminated from the database. At any one thermodynamic state with fixed pressure, Planck temperature and reference temperature, the mole fraction set of the third species may thus vary with the mole fractions of the other two species.

As a result, the retained mole fractions of a certain species vary with pressure, gas temperature and reference temperature and an index file recording these sets of retained mole fractions at different thermodynamic states is required. The sets of retained mole fractions for different thermodynamic states are stored in an ordered fashion according to their pressure, gas temperature and reference temperature. To employ dynamic loading, the offsets to retrieve the specific pre-stored k-values are also recorded in the index file. During calculations, the information of offsets and mole fractions at the required thermodynamic state is first loaded into memory, followed by the corresponding k-values. Since the size of the index file is only 7.4 MB, both computational cost and memory during calculations are only negligibly affected.

Table 1
Integral in Eq. (9) calculated by the tabulated a-values and the calculated a-values for a 10.0% CO_2–20% H_2O–70% N_2 mixture at 1 bar; 16-point quadrature.

Case	T (K)	T^0 (K)	Integral parts (m^{-1}) calculated by		Relative error (%)
			Tabulated a-values	Calculated a-values	
1	500	1000	5.797	5.640	2.71
2	1000	500	2.993	2.961	1.07
3	1500	2500	1.319	1.293	1.97
4	2500	1500	0.330	0.334	−1.21
5	2000	2500	0.637	0.623	2.20
6	2500	2000	0.333	0.335	−0.60

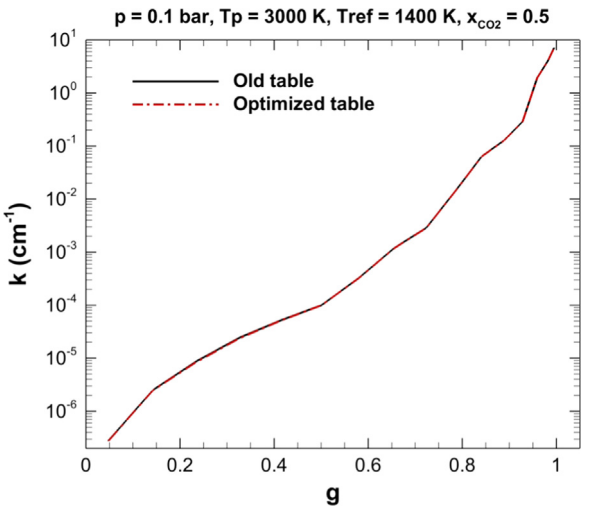

Fig. 1. *k*-Distributions calculated from old table and optimized table; 16-point quadrature.

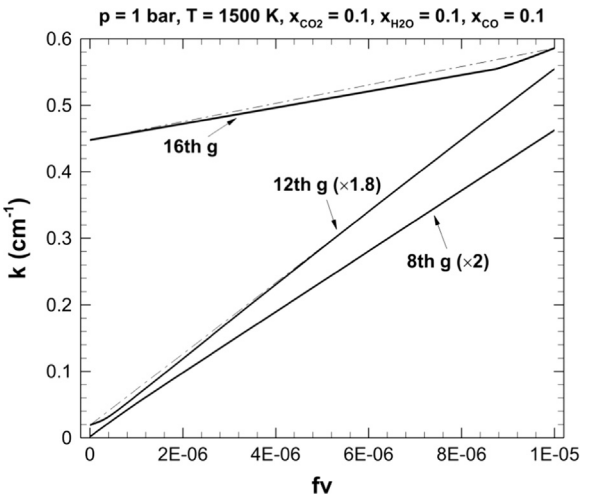

Fig. 2. Exact *k*-values corresponding to 8th, 12th and 16th *g*-quadrature values with the increasing volume fraction of soot using a 16-point Gauss–Chebyshev quadrature scheme [dash-dot lines represent the linear interpolation lines connecting the first and the last *k*-values; (× 2) and (× 1.8) imply amplification factors].

After optimization, the size of the FSK look-up table is reduced from 2.5 GB to 1.6 GB. Fig. 1 shows an example of a *k*-distribution of CO_2 obtained from the old table and from the optimized table at one thermodynamic state. The *k*-distributions from the old table are directly retrieved from the database without interpolation, while those from the optimized table are obtained by linear interpolation since there are only three mole fractions (0, 0.05, 1) remaining for CO_2 after optimization. The interpolated values from the optimized table show excellent agreement with those from the old table. This illustrates that the accuracy of the optimized table is almost unaffected.

3.2. Construction of the new table

To avoid the mixing process, the *k*-distribution of gas–soot mixtures is also generated directly from the mixture linear absorption coefficient for different thermodynamic states, which can be expressed as

$$\kappa_\eta = \left(x_{CO_2}\kappa_{p\eta\_CO_2} + x_{H_2O}\kappa_{p\eta\_H_2O} + x_{CO}\kappa_{p\eta\_CO}\right)\cdot p + \kappa_{\eta\_Soot} \qquad (11)$$

where, x_{CO_2}, x_{H_2O} and x_{CO} are the mole fractions of CO_2, H_2O and CO, respectively; p is the total pressure and the subscript 'p' represents the pressure-based absorption coefficient. Spectral absorption coefficients of soot can be calculated from Eq. (3).

The new table is constructed based on the optimized table in the previous section, and the approach to generate absorption coefficients and *k*-distributions has been given in [3], where details can be found. To determine the number of volume fractions of soot to be added, the nonlinear behavior of gas–soot mixture *k*-distributions with varying volume fractions of soot needs to be checked. Fig. 2 shows the exact *k*-values corresponding to different quadrature points with increasing volume fraction of soot at one thermodynamic state. Nonlinearities are observed for the 12th and 16th *g*-quadrature points as shown. However, compared to those of gas-only *k*-distributions, the nonlinearities of the *k*-distributions of gas–soot mixtures are relatively weak. For example, the maximum error between the exact value and the linear interpolation for the 16th *g*-quadrature point is only around 3%. For some quadrature points, like the 8th *g*-quadrature point, using linear interpolation can accurately represent the variation of the *k*-values with the volume fraction of soot; considering the volume fraction of soot is below 10 ppm in most combustion scenarios, only 1 volume fraction of soot (10 ppm) is included in the new table. For completeness, the pressures, gas temperatures, reference temperatures and volume fraction of soot in the new table are summarized in Table 2. The values of mole fractions for the three species depend on the selected thermodynamic state.

The size of the new table is 3.2 GB, i.e., double the size of the optimized table developed in Section 3.1. For every thermodynamic state, 32 *k*-values are stored in the database to guarantee the accuracy for most optical conditions. The same index file mentioned in Section 3.1 is also required for the implementation of dynamic loading. For an arbitrary thermodynamic state, the full-spectrum *k*-distribution is specified by pressure, gas temperature, reference temperature, three concentrations and soot. Therefore, a seven-dimensional linear interpolation method is required to obtain the full-spectrum *k*-distribution from the new table.

4. Flame calculations

To test the accuracy as well as efficiency of the new FSK look-up table, radiation from two realistic flames are considered. For both flames, only the quasi-steady time-average profiles are used for radiative calculation comparisons. Hence, no turbulence-radiation interaction is considered and the negative radiative heat source $\nabla\cdot q$ is determined using the LBL and the FSK methods without feedback to the flame. The RTE is solved by the P_1 method and the total pressure is 1 bar. All the FSK calculations

employ a 16-point Gauss–Chebyshev quadrature scheme obtained from the 32 database values using linear interpolation.

4.1. Nonluminous flame

The flame is derived from the Sandia Flame D [7] by artificially quadrupling the jet diameter, resulting in strong radiation effects that are found in practical combustion configurations. A two-dimensional axisymmetric mesh with 3325 cells is used for the simulation of the flame. The results using the narrow-band database [8] and the old table have been presented in [3], in which the flame profile of the temperature and the species mass fractions can be found. Since there is no soot in the flame, radiative calculations here are to verify the accuracy and the efficiency of the optimization described in Section 3.1. For the narrow-band database, the uncorrelated mixing model [9] is employed. As shown in Fig. 3, using the old table provides excellent performance compared to the LBL results. The discrepancies between the results from the old table and the LBL results mainly come from quadrature errors and interpolation errors due to the nonlinearities. For the narrow-band database, the process of mixing also results in some errors. Therefore, the results using the narrow-band database may be not as good as those using the old table, e.g., at location $z=1$ m. In the new table, a number of mole fractions were deleted after the optimization, resulting in an inevitable slight increase of interpolation error. The calculated a-values also provide another source of error due to the small number of the fixed g-values (for both the old and the new tables, only 32 fixed g-values were chosen). Therefore, calculations using the new table show slightly inferior performance compared to the results using both the narrow-band database and the old table. However, the discrepancies among the results using narrow-band database, old table and new table are barely seen from the lines of negative radiative heat source shown in Fig. 3 (right column), implying that the use of the new table also provides excellent accuracy in predicting the radiative heat source.

Table 2
Precalculated thermodynamic states of the new FSK look-up table.

Parameters	Range	Values	Number of points
Species	CO_2, H_2O, CO and soot		4
Pressure (total)	0.1–0.5 bar 0.7 bar 1.0–14.0 bar 15.0–80 bar	Every 0.1 bar 0.7 bar Every 1.0 bar Every 5 bar	34
Gas temperature	300–3000 K	Every 100 K	28
Reference temperature	300–3000 K	Every 100 K	28
Mole fraction of CO_2	0.0–1.0	[a]	[a]
Mole fraction of H_2O	0.0–1.0	[a]	[a]
Mole fraction of CO	0.0–0.5	[a]	[a]
Volume fraction of soot	0–10 ppm	[0 ppm, 10 ppm]	2

[a] Depends on the selected thermodynamic states.

Comparison of CPU times using different databases is shown in Table 3. Using the narrow-band database can save significant CPU time compared to the LBL calculations since the FSK method greatly reduces the number of the RTE evaluations. However, due to mixing and assembly, CPU time using the narrow-band database is still about 3 orders of magnitude higher than that using both the old and the new tables. For the calculations with feedback, it is quite time-consuming to use the narrow-band database in practical applications. CPU time for the new table is slightly shorter than that using the old table. The reason for this is that the a-values from the new table are directly calculated from the corresponding k-values with the 32 linear interpolations (1 linear interpolation is needed to get the a-value for each g-quadrature point); in contrast, to retrieve the a-values from the old table, 64 linear interpolations are required for one thermodynamic state with fixed pressure, Planck temperature, gas temperature and three

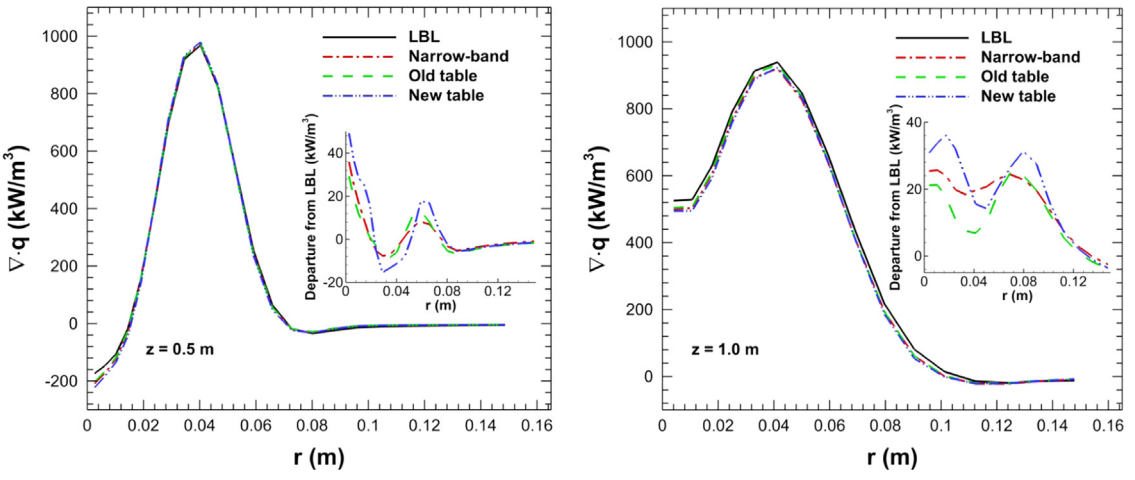

Fig. 3. Comparisons of negative radiative heat source calculations for Sandia Flame D × 4 using different spectral databases at two locations, $z=0.5$ m (left), $z=1.0$ m (right).

concentrations. Thus, use of the new table gives almost the same performance in accuracy and better performance in efficiency for radiation calculations in gaseous media.

4.2. Luminous flame

The luminous flame investigated here is the Flame VII in [10], which is also a scaled flame by enlarging the original jet diameter of 3 mm by a factor of 32. The flame is simulated on a two-dimensional axisymmetric mesh with 10,000 cells. The temperature, species mass fractions and soot volume fraction of the flame are shown in Fig. 4 and the peak soot volume fraction is around 8 ppm.

Results for the negative radiative heat source at two different locations are shown in Fig. 5. In the optically thin method, self-absorption by the medium is ignored in the calculations, so the results using this method only represent the total emission from the medium. At both locations, a large fraction of the emission is reabsorbed by the medium, illustrating strong radiation effects in this scaled flame. For the narrow-band database, the k-distributions are assembled from the narrow-band gas–soot mixture k-distributions, which are obtained by adding the average spectral soot absorption coefficient across the narrow-band to the gas k-distributions of that narrow-band. To guarantee accuracy, the uncorrelated mixing model is employed for the narrow-band database. Since the old table is only valid for gaseous media, the gas–soot mixture k-distributions from this table are calculated by directly adding the Planck mean absorption coefficient of soot to the gas-only k-distributions, i.e., the soot is treated as gray. For the new table, the gas–soot mixture k-distributions are directly obtained from the database by linear interpolation.

Table 3
Comparisons of CPU times for calculations of the Sandia Flame D × 4 case using different databases.

Database	CPU (s)
LBL	87332
Narrow-band	8423
Old table	1.56
New table	1.23

As seen from Fig. 5, the results using the narrow-band database show the best performance compared to the LBL results at both locations. The gas–soot mixture k-distributions from the old table are obtained by assuming the soot to be gray, which, as expected, leads to the worst performance among the three databases. At the location where the effects of self-absorption are strong ($z=4$ m), the maximum error between the LBL results and the old table results can be as much as 10%. By comparison, using the new table gives better results. Errors due to the non-linearities of k-distributions by using a single databased soot volume fraction, leads to less accurate results than using the narrow-band database, e.g., at location $z=2$ m. However, the differences between the narrow-band results and the new table results are relatively small, illustrating that the new table can also give accurate predictions for radiative calculations in the gas–soot mixtures. The Flame VII is an extreme case of a large flame with very strong soot formation and strong soot self-absorption, which is the cause for the small error incurred by using the old database with gray soot. For many combustion scenarios (and, indeed other parts of the Flame VII) self-absorption by soot is relatively small, and treating soot as gray should lead to accurate results.

Comparisons of CPU times using the different databases for the Flame VII are shown in Table 4. Since k-distributions are required for each cell during radiative calculations, the ratio of computational times for Flame VII and Sandia Flame D × 4 is roughly 3 when using the same database. Due to the assembly of k-distribution from individual species and mixing, the required CPU time for the narrow-band database, while large, is considerably lower than that calculated from the LBL database. Since more linear interpolations are required to retrieving the a-values from the database, using the old table requires a little more computational time than the new table. Therefore, together with the accuracy discussions above,

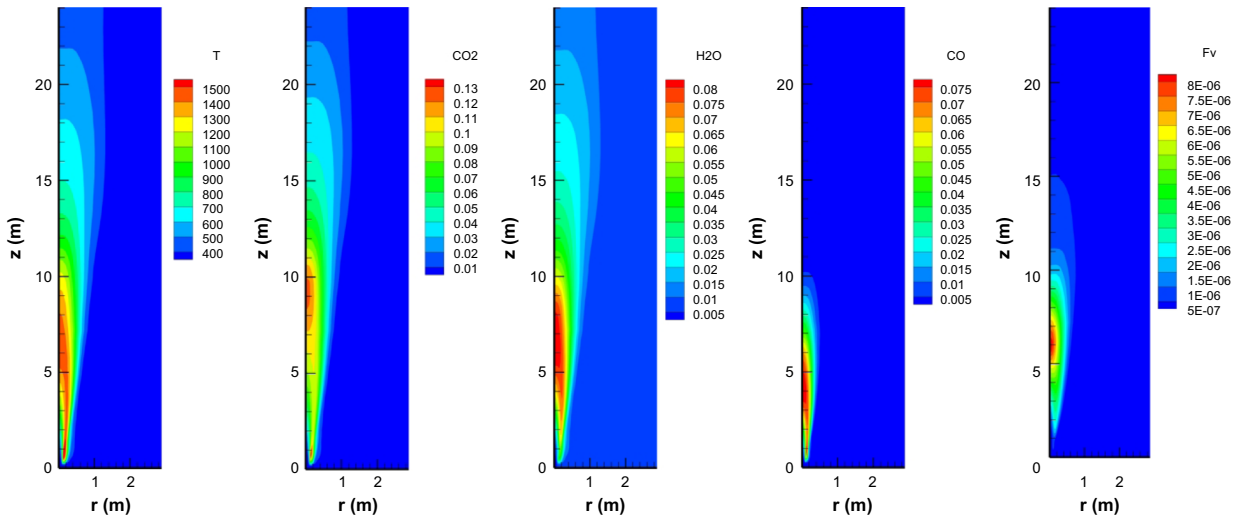

Fig. 4. Time-averaged spatial profile of temperature, CO_2 mass fraction, H_2O mass fraction, CO mass fraction and soot volume fraction of Flame VII.

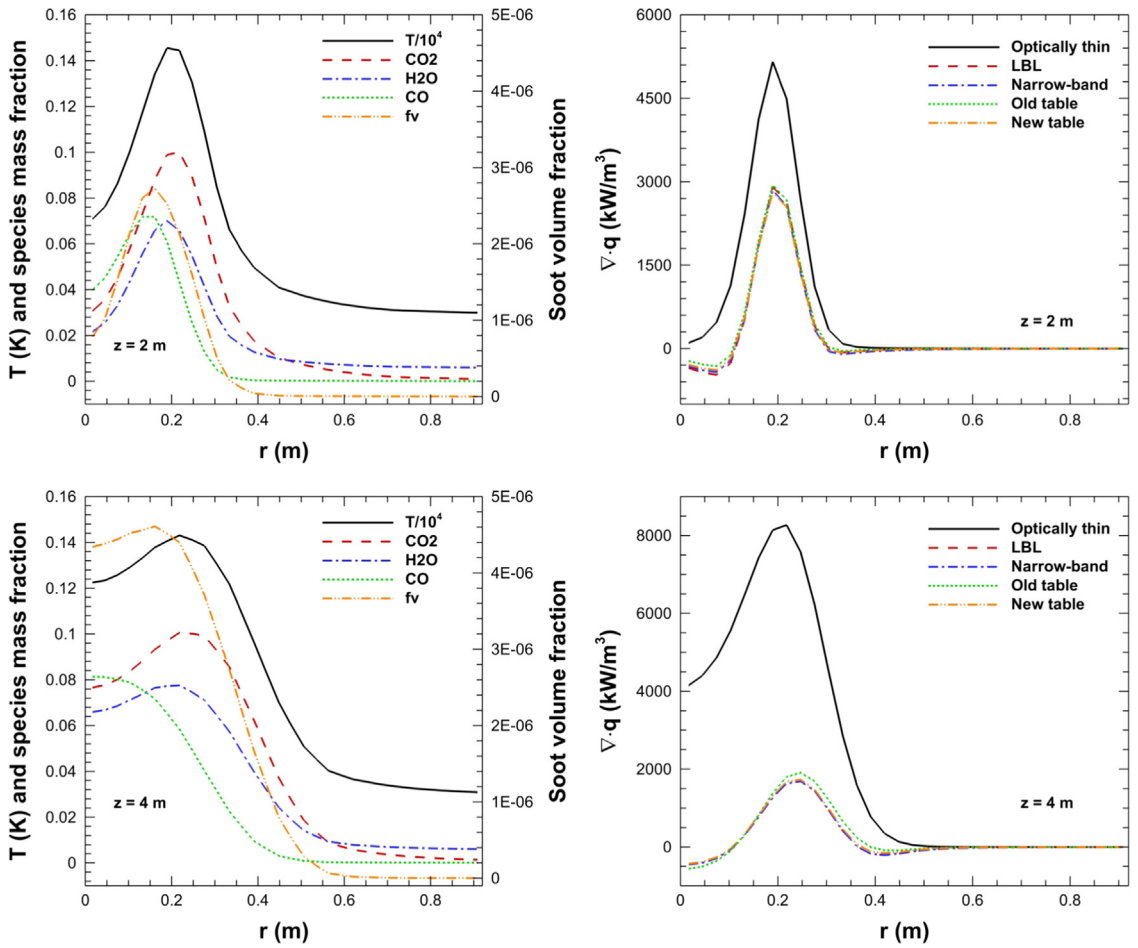

Fig. 5. Comparisons of negative radiative heat source calculations for the Flame VII using different spectral databases (right column) along with the temperature, the species mass fraction and the soot volume fraction (left column) at two locations, $z=2$ m (top), $z=4$ m (bottom).

Table 4
Comparisons of CPU times for calculations of the Flame VII case using different databases.

Database	CPU (s)
LBL	275322
Narrow-band	26027
Old table	5.06
New table	3.93

using the new table appears to be an excellent alternative for radiative calculations in the gas–soot mixtures.

5. Conclusions

To extend the applicability range of the recently published FSK look-up table, a new table has been constructed by optimizing the old table and then adding one soot volume fraction (10 ppm) to the optimized table. The optimization scheme is carried out in two steps. First the a-values are calculated on the fly instead of being tabulated; second, unnecessary mole fractions for different thermodynamic states were identified and deleted. Radiation from two realistic flames was considered to demonstrate the accuracy and the speed of the new table. Considering both the accuracy and the efficiency, the new table appears to be a very effective tool for both the gas-only and the gas–soot mixtures.

The new look-up database is available from the corresponding author's website upon request at http://eng.ucmerced.edu/people/mmodest.

Acknowledgments

This work was supported by the NSF/DOE Collaborative Research Award no. 1258635, and the China Scholarship Council.

References

[1] Arnold JO, Whiting EE, Lyle GC. Line-by-line calculation of spectra from diatomic molecules and atoms assuming a Voigt line profile. J Quant Spectrosc Radiat Transf 1969;9(6):775–98.
[2] Modest MF. Narrow-band and full-spectrum k-distributions for radiative heat transfer-correlated-k vs. scaling approximation. J Quant Spectrosc Radiat Transf 2003;76(1):69–83.

[3] Wang CJ, Ge WJ, Modest MF, He BS. A full-spectrum *k*-distribution look-up table for radiative transfer in nonhomogeneous gaseous media. J Quant Spectrosc Radiat Transf 2016;168:46–56.
[4] Modest MF, Riazzi RZ. Assembly of full-spectrum k-distributions from a narrow-band database; effects of mixing gases, gases and nongray absorbing particles, and mixtures with nongray scatterers in nongray enclosures. J Quant Spectrosc Radiat Transf 2005;90:169–89.
[5] Modest MF. In: Radiative heat transfer. 3rd ed.New York: Academic Press; 2013.
[6] Chang H, Charalampopoulos TT. Determination of the wavelength dependence of refractive indices of flame soot. In: Proceedings of the Royal Society, London; 1990. p. 577–91.
[7] Pal G, Gupta A, Modest MF, Haworth DC. Comparison of accuracy and computational expense of radiation models in simulation of non-premixed turbulent jet flames. In: Proceedings of the ASME/JSME 2011 8th thermal engineering joint conference. Honolulu, Hawaii, USA; Mar 13–17, 2011.
[8] Cai J, Modest MF. Improved full-spectrum *k*-distribution implementation for inhomogeneous media using a narrow-band database. J Quant Spectrosc Radiat Transf 2014;141:65–72.
[9] Modest MF, Riazzi RJ. Assembly of full-spectrum *k*-distributions from a narrow-band database: effects of mixing gases, gases and nongray absorbing particles, and mixtures with nongray scatterers in nongray enclosures. J Quant Spectrosc Radiat Transf 2005;90(2):169–89.
[10] Mehta RS, Modest MF, Haworth DC. Radiation characteristics and turbulence-radiation interactions in sooting turbulent jet flames. Combust Theory Model 2010;14(1):105–24.